

# Thin Metal Electrodes for Semitransparent Organic Photovoltaics

Kyu-Sung Lee, Inho Kim, Chang Bong Yeon, Jung Wook Lim,  
Sun Jin Yun, and Ghassan E. Jabbour

**We demonstrate semitransparent organic photovoltaics (OPVs) based on thin metal electrodes and polymer photoactive layers consisting of poly(3-hexylthiophene) and [6,6]-phenyl C<sub>61</sub> butyric acid methyl ester. The power conversion efficiency of a semitransparent OPV device comprising a 15-nm silver (Ag) rear electrode is 1.98% under AM 1.5-G illumination through the indium-tin-oxide side of the front anode at 100 mW/cm<sup>2</sup> with 15.6% average transmittance of the entire cell in the visible wavelength range. As its thickness increases, a thin Ag electrode mainly influences the enhancement of the short circuit current density and fill factor. Its relatively low absorption intensity makes a Ag thin film a viable option for semitransparent electrodes compatible with organic layers.**

**Keywords:** Thin metal electrodes, semitransparent, organic photovoltaics.

Manuscript received Dec. 13, 2012; revised June 11, 2013; accepted June 19, 2013.

This work was partially supported by the New and Renewable Energy of the Korea Institute of Energy Technology Evaluation and Planning (KETEP) grant funded by the Korea Ministry of Knowledge Economy (Nos. 20118520010040 and 20123010010150).

Kyu-Sung Lee (phone: +82 42 860 5739, kysung.lee@etri.re.kr) was with the School of Engineering for Matter, Transport, and Energy (SEMTE), Arizona State University (ASU), Tempe, AZ, USA, and is now with the Components & Materials Research Laboratory, ETRI, Daejeon, Rep. of Korea.

Inho Kim (inhok@kist.re.kr) was with the SEMTE, ASU, Tempe, AZ, USA, and is now with the Electronic Materials Research Center, KIST, Seoul, Rep. of Korea.

Chang Bong Yeon (chbz@etri.re.kr), Jung Wook Lim (limjw@etri.re.kr), and Sun Jin Yun (sjyun@etri.re.kr) are with the Components & Materials Research Laboratory, ETRI, Rep. of Korea, and also with the Department of Advanced Device Engineering, University of Science and Technology, Daejeon, Rep. of Korea.

Ghassan E. Jabbour (jabbour@kaust.edu.sa) was with the SEMTE, ASU, AZ, USA, and is now with the Solar and Alternative Energy Engineering Research Center, King Abdullah University of Science and Technology, Thuwal, Kingdom of Saudi Arabia.

<http://dx.doi.org/10.4218/etrij.13.1912.0025>

## I. Introduction

Organic photovoltaic (OPV) cells are promising candidates for various power generating applications, and their recent progress shows ascending power conversion efficiency (PCE) of up to 10.6% based on a tandem structure [1]. It is thought that the manufacturing processes of OPV cells are more cost-effective than those of crystalline silicon solar cells and inorganic thin film solar cells by minimizing the vacuum deposition process [1]-[3]. The flexibility of substrates using plastic films, stainless steel foil, and even paper is also considered a unique advantage of OPV devices [3], [4]. The ultra-thinness and absorption band tunability of OPV photoactive layers enable the development of transparent and colorful PV products for power-generating windows of building-integrated photovoltaics and automatic vehicles [5]-[9].

To enhance the transparency of OPV electrodes for various applications, different approaches have been reported. Transparent conducting oxides, conducting polymers, carbon nanotubes, metal nanowires, graphene, thin metals, and combinations of these materials have been introduced in OPV devices with improving efficiencies [4], [7]-[13]. Conducting polymers, metal nanowires, and thin metals have shown desirable compatibility with organic photoactive layers. However, consecutive solution-processed electrodes on polymer layers might result in the dissolution of bottom photoactive layers or provide differences in wettability between polymers and electrode materials [10]. In this study, thin metal electrodes as top cathodes are investigated to achieve higher PCE of semitransparent OPV devices without solvent damage or a wettability issue of the bottom organic layers.

## II. Experiments

Thin metal films of aluminum (Al), gold (Au), and silver (Ag) are deposited onto glass substrates with a nominal thickness of 15 nm to compare their optical properties. The deposition rate and thickness are controlled using a quartz crystal thickness monitor. The transmittance (%*T*), reflectance (%*R*), and absorbance (%*A*) spectra of metal thin films are obtained using a UV-visible spectrophotometer with a diffuse reflectance accessory in air. Each semitransparent OPV cell has a front side with an indium-tin-oxide (ITO) thin film and a rear side with a Ag thin film. The optical spectra of each semitransparent OPV cell are measured at both the front side (ITO, 150 nm) and the rear side (Ag, 15 nm). The average %*T* is calculated for visible wavelengths from 400 nm to 750 nm. The thin Ag films employ different thicknesses, and the sheet resistance ( $R_{\text{sheet}}$ ) of each thin Ag film is measured using the four-point probe method. Surface images of thin Ag films and root-mean-square roughness ( $R_{\text{rms}}$ ) are measured using a scanning probe microscope (SPM) with a scan area of 4  $\mu\text{m}^2$ .

Semitransparent OPV devices are fabricated using solution processes on ITO-coated glasses. All substrates are cleaned, followed by surface treatments using a UV ozone cleaner prior to the spin-coating steps. Hole transporting layers of poly(3,4-ethylenedioxythiophene):poly(styrenesulfonate) (PEDOT:PSS, 40 nm) are spin-coated and dried at 150°C for 30 minutes. Poly(3-hexylthiophene) (P3HT, 30 mg) and [6,6]-phenyl C<sub>61</sub> butyric acid methyl ester (PCBM, 24 mg) for the photoactive layers are mixed in 1,2-dichlorobenzene (DCB, 1 ml) for 12 hours. Spin-coated photoactive layers (250 nm) are dried at 150°C for 30 minutes on a hot plate to remove residual solvents and stabilize the polymer networks. Bathocuproine (BCP, 15 nm) as an exciton blocking layer and thin metals as cathodes are thermally evaporated in a vacuum chamber at a

base pressure of  $1 \times 10^{-7}$  Torr at room temperature.

The current density-voltage (*J-V*) characteristics are obtained using a source measure unit under AM 1.5-G illumination through the ITO side of the front anode at 100 mW/cm<sup>2</sup>. The device fabrication steps and *J-V* measurements of the OPV devices are processed in nitrogen glove boxes. Their external quantum efficiencies (EQEs) and internal quantum efficiencies (IQEs) are evaluated in air at wavelengths of 350 nm to 700 nm through the front side (ITO) illumination.

## III. Results and Discussion

Optical spectra of various thin metal films are compared in Figs. 1(a) through 1(c). A reflective electrode of 80-nm Ag film is also compared with 15-nm Al, Au, and Ag films on glass substrates. The absorption intensity (%*A* = 100% - %*T* - %*R*) of the 15-nm Al and Au films is higher than that of the 15-nm Ag thin film and can limit the use of Al and Au thin metal electrodes as semitransparent applications, as shown in Fig. 1(c). Accordingly, semitransparent Ag film is considered the best combination of optical and conductive aspects in optoelectronic devices [13]. The overall %*T* of 15 nm in the Ag films is more than 40%, which is higher than the transmittance values of other thin metals, indicating that a thin Ag electrode is a fitting candidate for a semitransparent electrode at visible wavelengths.

Since the transparency of the whole device is an important factor for semitransparent applications, the optical properties are further investigated to compare with a variation in Ag thickness. The transmission spectra of Ag thin films on glass substrates employing different thicknesses are shown in Fig. 2. The average %*T* values of Ag thin films on glass substrates are gradually reduced from 52.3% to 34.5% with increments of the Ag thickness, as noted in Table 1, which facilitates the control

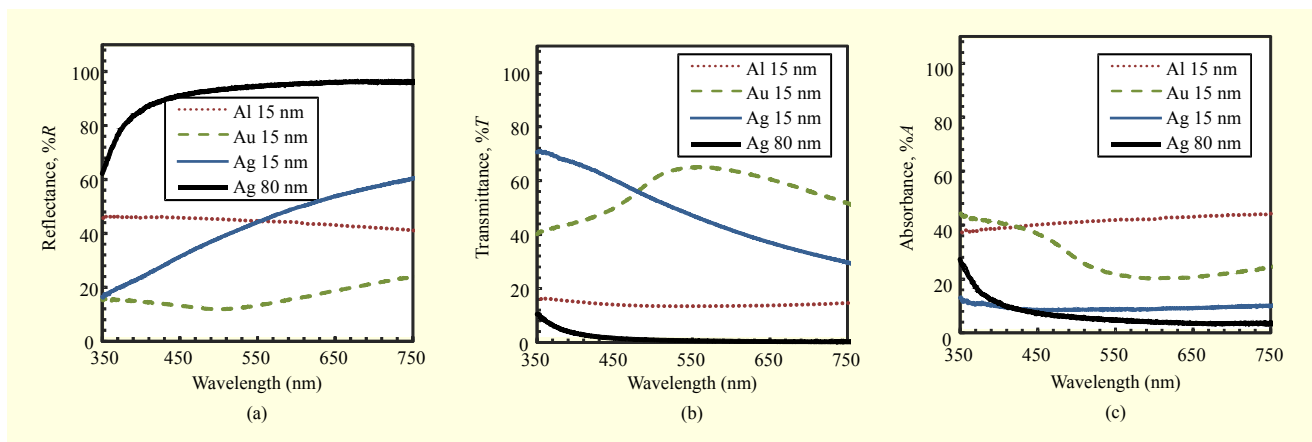


Fig. 1. (a) Reflection, (b) transmission, and (c) absorption spectra of 15-nm semitransparent Al, Au, and Ag thin films compared with 80-nm reflective Ag film on glass substrates.

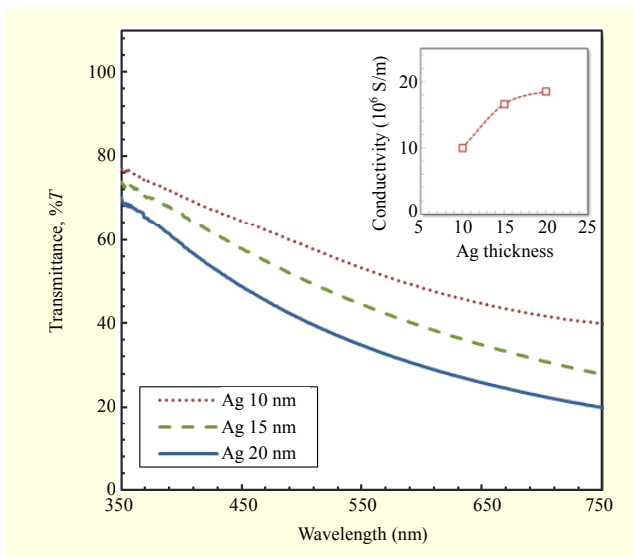


Fig. 2. Transmission spectra of semitransparent Ag thin films employing different thicknesses. Inset shows calculated conductivity of Ag thin films.

Table 1. Average % $T$  values within visible range of 400 nm to 750 nm and  $R_{\text{sheet}}$  values for Ag thin films employing different Ag thicknesses.

	Ag 10 nm	Ag 15 nm	Ag 20 nm
Average % $T$	52.3	43.5	34.5
$R_{\text{sheet}}$ ( $\Omega/\text{sq}$ )	10.0	4.0	2.7

of transparency for use in tinted windows. High  $R_{\text{sheet}}$  of a 10-nm Ag layer can partially support the tendency of high series resistance ( $R_s$ ) of an OPV device owing to a low conductivity calculated by the  $R_{\text{sheet}}$  and film thickness, as shown in the inset of Fig. 2. As described above, thin metal electrodes of a semitransparent OPV device show a tradeoff between optical transparency and electrical charge collection.

Overall, a semitransparent OPV device with a 15-nm Ag electrode is considered a viable option for a semitransparent window application with an average % $T$  of 43.5% and a  $R_{\text{sheet}}$  value of 4.0  $\Omega/\text{sq}$ , as shown in Table 1. The visible light transmittance of an OPV device is also affected by the absorption wavelengths and intensities of the photoactive layer. Although it would be different from the real Ag thin films on P3HT:PCBM organic photo-active layer, the transmittance and the conductivity of Ag thin film on a glass substrate can give an insight into or tendency of optical and electrical properties of Ag thin films. The average % $T$  values and the  $R_{\text{sheet}}$  values of Ag thin films employing different Ag thicknesses are summarized in Table 1.

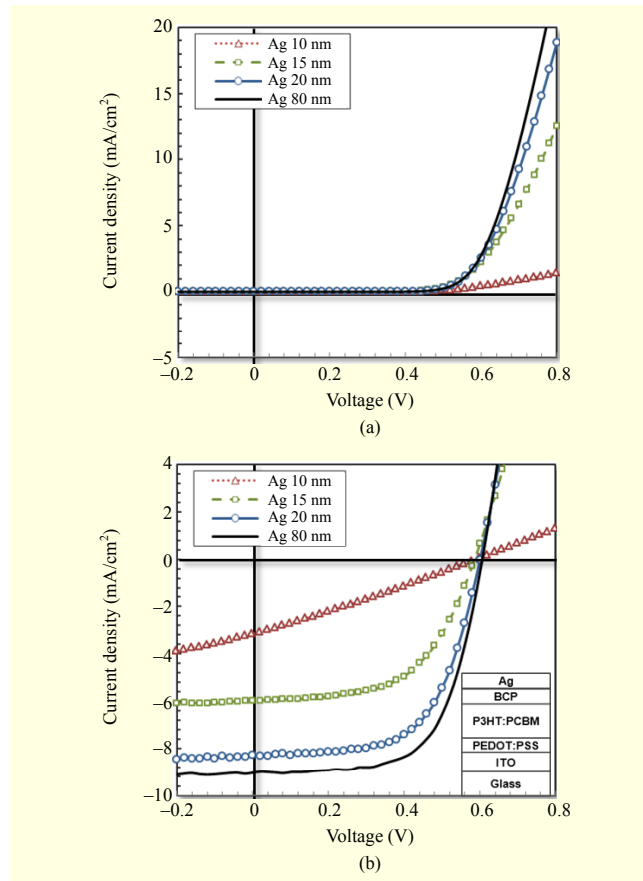


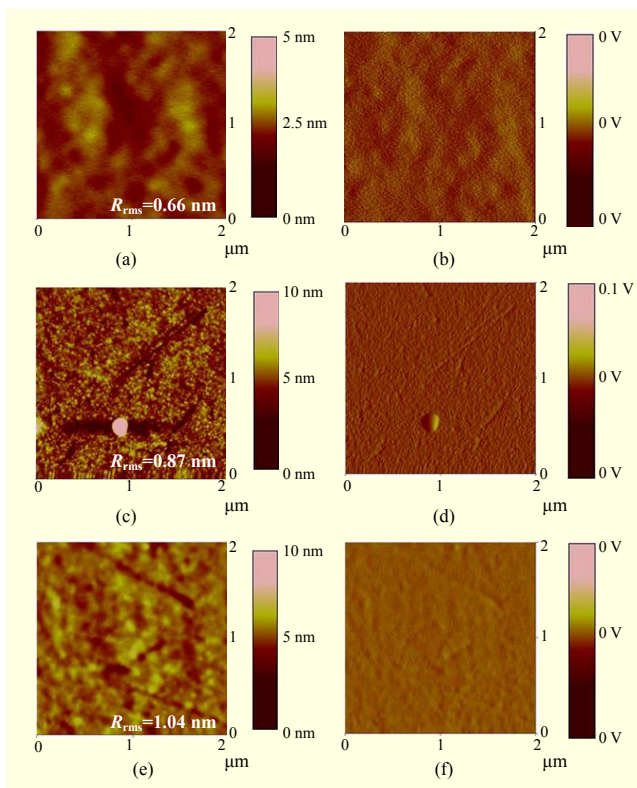
Fig. 3.  $J$ - $V$  characteristics of OPV devices comprising Ag electrodes with different thicknesses (a) dark and (b) illumination through ITO-side. Inset of (b) shows structure of OPV device.

Figure 3 shows typical  $J$ - $V$  characteristics of OPV devices consisting of 250-nm-thick P3HT:PCBM photoactive layers and various semitransparent Ag electrodes with different thicknesses and the reflective Ag electrode at dark and AM 1.5-G illumination. The device structure of this work is shown in the inset of Fig. 3(b). The open-circuit voltage ( $V_{\text{oc}}$ ) values of these devices are similar for all semitransparent OPV devices, regardless of the cathode thickness. In the case of OPV devices, the  $V_{\text{oc}}$  is related to either work function difference between the respective electrodes or energy level difference between the highest occupied molecular orbital of donors and the lowest unoccupied molecular orbital of acceptors [14]. Thus, aside from the thickness variation, the identical device structure of semitransparent OPVs in this work contributes to the  $V_{\text{oc}}$  results being without dramatic changes.

On the other hand, the short-circuit current density ( $J_{\text{sc}}$ ) and fill factor (FF) show significant differences in Fig. 3. These device parameters are strongly dependent on the thickness of the semitransparent Ag electrodes, resulting in changes in the PCEs. The device parameters of OPV devices with different

**Table 2.** Device parameters of OPV devices comprising Ag electrodes with different thicknesses through ITO-side illumination.

Cathode	Ag 10 nm	Ag 15 nm	Ag 20 nm	Ag 80 nm
PCE (%)	0.50	1.98	3.03	3.49
$J_{sc}$ (mA/cm <sup>2</sup> )	3.14	5.98	8.29	9.04
$V_{oc}$ (V)	0.59	0.59	0.60	0.61
FF (%)	27.06	56.46	61.04	63.67
$R_s$ ( $\Omega\text{cm}^2$ )	153.86	13.53	8.05	5.91
Average % $T$	19.9%	15.6%	11.9%	-



**Fig. 4.** SPM surface images of Ag films on glass substrates. Height images of Ag thin films employing (a) 10 nm, (c) 15 nm, and (e) 20 nm and amplitude images of Ag thin films employing (b) 10 nm, (d) 15 nm, and (f) 20 nm.

Ag electrodes are summarized in Table 2. In addition, average % $T$  values of semitransparent OPV cells employing different thin Ag electrodes are calculated in visible wavelengths from 400 nm to 750 nm. Although a smaller photo-generated current of a semitransparent OPV device is mainly influenced from the lesser reflectivity of metal electrodes [5], an unfavorable increment in the  $R_s$  of an OPV device employing a 10-nm Ag electrode is possibly involved in a low charge collection efficiency with smaller FF. It has been

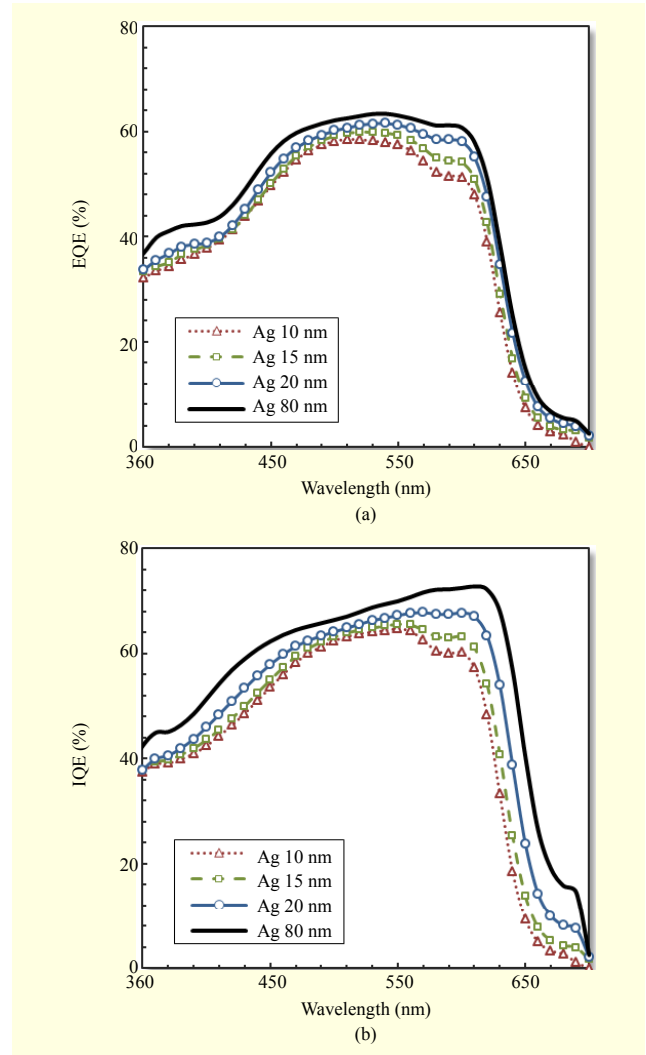


**Fig. 5.** (a) EQEs and (b) IQEs of OPV devices employing Ag electrodes with different thicknesses through ITO-side illumination.

reported that thin metal films have exhibited low conductivity owing to electron scattering and the formation of remaining voids [13], [15].

In Figs. 4(a) through 4(f), surface height and amplitude images of deposited Ag thin films with different thickness on glass substrates are shown. Roughness values ( $R_{rms}$ ) of these films exploit the smooth surfaces for all semitransparent Ag thin electrodes. The  $R_{rms}$  value of 15-nm Ag thin film is determined by excluding the particle region in Fig. 4(c). However, the surface morphology of 250-nm P3HT:PCBM photoactive layers may be rough, making it difficult to form a fully covered continuous thin metal electrode layer for 10-nm Ag films, leading to a specifically higher  $R_s$  and, in turn, a lower FF of the semitransparent OPV device. The dark  $J-V$  characteristics may support the conductivity tendency of semitransparent Ag thin films, as shown in Fig. 3(a). The dark



$J$ - $V$  curve of a device with a 10-nm Ag electrode shows a significant decrease in the slope of the linear regime due to rather disconnected ultra-thin Ag surfaces.

It is reported that 15-nm Ag thin film is almost a coalescence threshold for continuously connected networks and becomes much rougher on the organic layer [16], [17]. For this reason, the formation of fully covered semitransparent thin Ag films, such as 15-nm and 20-nm Ag thin films, can improve the charge collection at the interface between the photoactive layer and thin Ag electrode, leading to a better device performance. The improvement of  $J_{sc}$  from a semitransparent OPV device with a Ag electrode can be further explained with the results of the EQE and the IQE, as presented in Fig. 5.

As the thickness of a Ag electrode increases, the EQEs and IQEs are observed to have similar increments, leading to a higher  $J_{sc}$ . Due to this tendency of EQEs, the PCEs of OPV devices consisting of 20-nm-thick and 80-nm-thick Ag electrodes with a nearly saturated  $J_{sc}$  are comparable as 3.03% and 3.49%, respectively. However, the EQE results are not directly converted to  $J_{sc}$  of  $J$ - $V$  curves in Fig. 3 due to the charge collection issues, especially in the case of an OPV device with a 10-nm Ag electrode. Regarding the IQE results, the use of a semitransparent Ag electrode shows the possibility of more optical effects than reflective Ag films due to the distinctive changes in the wavelength ranges between 550 nm and 650 nm for the absorption ranges of a P3HT:PCBM photoactive layer, as shown in Fig. 5(b).

Figure 6 shows the transmission and reflection spectra of a semitransparent OPV device with a 15-nm Ag electrode when separately measured at both the ITO side of the front anode and Ag side of the rear cathode, respectively. That is, in this structure, the reflectance of the cell measured from the rear side

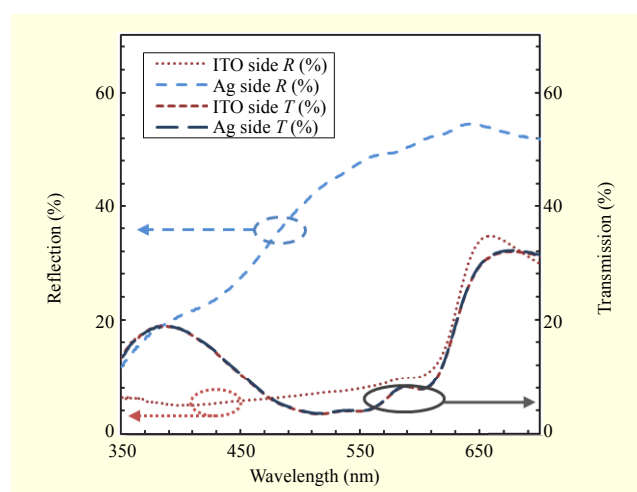


Fig. 6. Reflection and transmission spectra of OPV device with 15-nm Ag electrodes for front side (ITO) and rear side (Ag) measurements.

is much higher than the reflectance from the front side due to the optical asymmetry [9], whereas the % $T$  values of both sides are the same, proposing additional requirements for the anti-reflective coatings or a combination of other conducting materials to further improve the optical characteristics. Thus, a semitransparent OPV device with a 15-nm Ag rear electrode and a 250-nm P3HT:PCBM photoactive layer shows 1.98% PCE through ITO-side illumination and 15.6% average % $T$ , calculated by the results of Fig. 6.

#### IV. Conclusion

In summary, semitransparent organic photovoltaic devices were fabricated using solution-processed photoactive layers and thin metal electrodes. The device characteristics were investigated for both their optical and electrical aspects. The power conversion efficiency of a semitransparent OPV device with a 15-nm Ag electrode and 250-nm P3HT:PCBM photoactive layer was 1.98% through ITO-side illumination, with 43.5% and 15.6% average transmittance values for Ag thin films and a whole semitransparent OPV device, respectively. A combination of effective optical transparency and efficient electrical contacts of thin metal electrodes demonstrated the possibility to expand the applications of semitransparent OPV devices.

#### References

- [1] G. Li, R. Zhu, and Y. Yang, "Polymer Solar Cells," *Nature Photonics*, vol. 6, Mar. 2012, pp. 153-161.
- [2] N.-M. Park, H.S. Lee, and J. Kim, "Reactive Sputtering Process for  $\text{CuIn}_{1-x}\text{Ga}_x\text{Se}_2$  Thin Film Solar Cells," *ETRI J.*, vol. 34, no. 5, Oct. 2012, pp. 779-782.
- [3] S.-I. Na et al., "Efficient and Flexible ITO-Free Organic Solar Cells Using Highly Conductive Polymer Anodes," *Adv. Mater.*, vol. 20, no. 21, Nov. 2008, pp. 4061-4067.
- [4] F.C. Krebs, "Roll-to-Roll Fabrication of Monolithic Large-Area Polymer Solar Cells Free from Indium-Tin-Oxide," *Solar Energy Mater. Solar Cells*, vol. 93, no. 9, Sept. 2009, pp. 1636-1641.
- [5] R.F. Bailey-Salzman, B.P. Rand, and S.R. Forrest, "Semitransparent Organic Photovoltaic Cells," *Appl. Phys. Lett.*, vol. 88, no. 23, June 2006, pp. 233502.1-233502.3.
- [6] F.-C. Chen et al., "Polymer Photovoltaic Devices with Highly Transparent Cathodes," *Organic Electron.*, vol. 9, no. 6, Dec. 2008, pp. 1132-1135.
- [7] K.-S. Chen et al., "Semi-transparent Polymer Solar Cells with 6% PCE, 25% Average Visible Transmittance and a Color Rendering Index Close to 100 for Power Generating Window Applications," *Energy Environ. Sci.*, vol. 5, no. 11, Aug. 2012, pp. 9551-9557.
- [8] J.-Y. Lee et al., "Semitransparent Organic Photovoltaic Cells with

Laminated Top Electrode,” *Nano Lett.*, vol. 10, no. 4, Mar. 2010, pp. 1276-1279.

- [9] D. Han et al., “Realization of Efficient Semitransparent Organic Photovoltaic Cells with Metallic Top Electrodes: Utilizing the Tunable Absorption,” *Opt. Express*, vol. 18, no. S4, Nov. 2010, pp. A513-A521.
- [10] V. Shrotriya et al., “Efficient Light Harvesting in Multiple-Device Stacked Structure for Polymer Solar Cells,” *Appl. Phys. Lett.*, vol. 88, no. 6, Feb. 2006, pp. 064104.1-064104.3.
- [11] J. van de Lagemaat et al., “Organic Solar Cells with Carbon Nanotubes Replacing  $\text{In}_2\text{O}_3:\text{Sn}$  as the Transparent Electrode,” *Appl. Phys. Lett.*, vol. 88, no. 23, June 2006, pp. 221008.1-221008.3.
- [12] X. Wang, L. Zhi, and K. Müllen, “Transparent, Conductive Graphene Electrodes for Dye-Sensitized Solar Cells,” *Nano Lett.*, vol. 8, no. 1, Dec. 2008, pp. 323-327.
- [13] B. O’Connor et al., “Transparent and Conductive Electrodes Based on Unpatterned, Thin Metal Films,” *Appl. Phys. Lett.*, vol. 93, no. 22, Dec. 2008, pp. 223304.1-223304.3.
- [14] M.C. Scharber et al., “Design Rules for Donors in Bulk-Heterojunction Solar Cells-Towards 10% Energy-Conversion Efficiency,” *Adv. Mater.*, vol. 18, no. 6, Mar. 2006, pp. 789-794.
- [15] P. Zhao et al., “Properties of Thin Silver Films with Different Thickness,” *Physica E*, vol. 41, no. 3, Jan. 2009, pp. 387-390.
- [16] J. Meiss, M.K. Riede, and K. Leo, “Optimizing the Morphology of Metal Multilayer Films for Indium Tin Oxide (ITO)-Free Inverted Organic Solar Cells,” *Appl. Phys. Lett.*, vol. 105, no. 6, Mar. 2009, pp. 063108.1-063108.3.
- [17] H.B. Yang et al., “New Architecture for Accurate Characterization of the Behavior of Individual Sub-Cells within a Tandem Organic Solar Cell,” *Energy Environ. Sci.*, vol. 1, no. 3, June 2008, pp. 389-394.



**Kyu-Sung Lee** received his BS and MS in materials science and engineering from Seoul National University, Seoul, Rep. of Korea, in 2001 and 2003. He earned his PhD in materials science and engineering from Arizona State University (ASU), Tempe, AZ, USA, in 2012. From 2003 to 2008, he was a research engineer at Samsung SDI. Co. Ltd. Since he joined ETRI, Daejeon, Rep. of Korea, in 2012, he has been working for the Solar Cell Technology Research Team. His research interests are optoelectronic devices, transparent electrodes, and nanostructured and nanomaterials-/silicon-based solar cells.



**Inho Kim** is a senior researcher at the Electronic Materials Research Center in the Korea Institute of Science and Technology (KIST), Seoul, Rep. of Korea. He received his BE from Seoul National University, Seoul, Rep. of Korea, his ME from the Korea Advanced Institute of Science and Technology (KAIST), Daejeon, Rep. of Korea, and his PhD from Arizona State University (ASU), Tempe, AZ, USA. His research interests are design and fabrication of nanostructures for light trapping in photovoltaics and plasmonic-based chemical sensors.



**Chang Bong Yeon** received his BS in chemistry from Chungnam National University, Daejeon, Rep. of Korea, in 2011 and his MS in advanced materials and devices from the University of Science and Technology, Daejeon, Rep. of Korea, in 2013. He was a researcher in the research center of the Korea Chemical Corporation in 2013. His current research interest is transparent conducting oxides using graphene.



**Jung Wook Lim** received his BS, MS, and PhD from the Korea Advanced Institute of Science and Technology (KAIST), Daejeon, Rep. of Korea, in 1994, 1996, and 2001, respectively. He has been with ETRI, Daejeon, Rep. of Korea, since 2001. Also, he has been a professor with the Department of Advanced Device Engineering at the University of Science and Technology, Daejeon, Rep. of Korea, since 2006. He has conducted research in the fields of atomic layer deposition and Si thin film solar cell technology. His current research interests include transparent thin film solar cells and silicon heterojunction solar cells.



**Sun Jin Yun** received her BS in chemistry from Pusan National University, Busan, Rep. of Korea, in 1982 and her MS and PhD in physical chemistry from the Korea Advanced Institute of Science and Technology (KAIST), Seoul, Rep. of Korea, in 1983 and 1987, respectively. Since 1987, she has worked for ETRI, Daejeon, Rep. of Korea. Also, from 1992 to 1993, she worked as a visiting research associate with the Department of Electrical and Computer Engineering at the University of Illinois, Urbana-Champaign, IL, USA. Since 2006, she has also been a professor with the Department of Advanced Device Engineering of the University of Science and Technology, Daejeon, Rep. of Korea. Her research interests include the fabrication of new functional thin films and the development of inorganic thin film photovoltaic cells, sensors, and microelectronic devices utilizing

engineered thin films.



**Ghassan E. Jabbour** is the director of the Solar and Alternative Energy Science and Engineering Research Center at King Abdullah University of Science and Technology, Thuwal, Saudi Arabia. He was the director of the Advanced Photovoltaics Center, the director optoelectronics research for the Flexible Display Center (FDC), and a professor of chemical and materials engineering at Arizona State University (ASU), Tempe, AZ, USA. His research experience encompasses flexible roll-to-roll electronics and displays, smart textiles, moisture and oxygen barrier technology, transparent conductors, organic light-emitting devices, organic and hybrid photovoltaics, organic memory storage, organic thin-film transistors, combinatorial discovery of materials, nanoprinted and macroprinted devices, microfabrication and nanofabrication, biosensors, and quantum simulations of electronic materials. He attended Northern Arizona University, Flagstaff, AZ, USA, the Massachusetts Institute of Technology (MIT), Cambridge, MA, USA, and the University of Arizona, Tucson, AZ, USA.